Chapter 2
Oxidation of Alcohols Catalyzed by Supported Undecamolybdophosphate

Abstract Synthesis and stabilization of undecamolybdophosphate (PMo_{11}) as well as its characterization was explained. Also, synthesis and characterization of series of heterogeneous catalysts comprising PMo_{11} and different supports (ZrO_2, Al_2O_3, MCM-41 and zeolite-Hβ) and their use as heterogeneous catalysts for solvent free oxidation of alcohols with molecular oxygen and TBHP as a radical initiator was described. The influence of different parameters on the conversion as well as the selectivity was investigated on oxidation of benzyl alcohol. Further, oxidation of various alcohols such as cyclopentanol, 1-hexanol and 1-octanol over supported PMo_{11} was presented under optimized conditions. All the catalysts are found to be efficient especially in achieving higher selective toward desire product and high turnover numbers. Regeneration study showed that the catalysts can be regenerated and reused without any significant loss in the catalytic activity.

Keywords Undecamolybdophosphate · Metal oxides · Porous silica · Oxidation · Alcohols

2.1 Undecamolybdophosphate Supported on to Metal Oxides (ZrO_2, Al_2O_3)

2.1.1 Experimental

All the chemicals used were of A. R. grade. Sodium molybdate, Disodium hydrogen phosphate, zirconium oxychloride, liquor ammonia, neutral active Al_2O_3 (Activity I–II, according to Brockmann), Nitric acid, acetone, benzyl alcohol, cyclopentanol, cyclohexanol, 1-hexanol, 1-octanol, tertiary butylhydroperoxide (70 % aq. TBHP) and dichloromethane were obtained from Merck and used as received.

A. Patel and S. Pathan, *Polyoxomolybdates as Green Catalysts for Aerobic Oxidation*, SpringerBriefs in Green Chemistry for Sustainability,
DOI 10.1007/978-3-319-12988-4_2

2.1.1.1 Synthesis of Na Salt of Undecamolybdophosphate (PMo_{11}) [1]

Sodium molybdate dihydrate (0.22 mol, 5.32 g) and anhydrous disodium hydrogen phosphate (0.02 mol, 0.28 g) were dissolved in 50–70 mL of conductivity water and heated to 80–90 °C followed by the addition of concentrated nitric acid in order to adjust the pH to 4.3. The volume was then reduced to half by evaporation and the heteropolyanion was separated by liquid–liquid extraction with 50–60 mL of acetone. The extraction was repeated until the acetone extract showed absence of NO_3^- ions (ferrous sulfate test). The extracted sodium salt was dried in air. The obtained sodium salt of undecamolybdophosphate was designated as PMo_{11}.

2.1.1.2 Synthesis of Supported Catalysts

Synthesis of the support, ZrO_2
Hydrous zirconia was prepared by adding an aqueous ammonia solution to an aqueous solution of $ZrOCl_2 \cdot 8H_2O$ up to pH 8.5. The precipitates were aged at 100 °C over a water bath for 1 h, filtered, washed with conductivity water until chloride free water was obtained and dried at 100 °C for 10 h. The obtained material is designated as ZrO_2.

Supporting of PMo_{11} onto ZrO_2 (PMo_{11}/ZrO_2) [1]
PMo_{11} was supported on ZrO_2 by dry impregnating method. 1 g of ZrO_2 was impregnated with an aqueous solution of PMo_{11} (0.1 g/10 mL of double distilled water). The water from the suspension was allowed to evaporate at 100 °C in an oven. Then the resulting mixture was dried at 100 °C with stirring for 10 h. The material thus obtained was designated as 10 % PMo_{11}/ZrO_2. Same procedure was followed for the synthesis of a series of supported PMo_{11} containing 20–40 % PMo_{11} (0.2–0.4 g/20–40 mL of conductivity water). The obtained materials were designated as 20 % PMo_{11}/ZrO_2, 30 % PMo_{11}/ZrO_2 and 40 % PMo_{11}/ZrO_2 respectively.

Supporting of PMo_{11} onto Al_2O_3 (PMo_{11}/Al_2O_3) [2]
A series of catalysts containing 10–40 % PMo_{11} were synthesized by impregnating 1 g of Al_2O_3 with an aqueous solution of PMo_{11} (0.1–0.4 g in 10–40 mL of conductivity water) with stirring for 35 h and then dried at 100 °C for 10 h. The obtained materials were designated as 10 % PMo_{11}/Al_2O_3, 20 % PMo_{11}/Al_2O_3, 30 % PMo_{11}/Al_2O_3 and 40 % PMo_{11}/Al_2O_3.

2.1.1.3 Characterization

Characterization is a central aspect of catalyst development. The elucidation of the structures, compositions, and chemical properties of both the supports used in

heterogeneous catalysis as well as the active species present on the surfaces of the supported catalysts is very important for a better understanding of the relationship between catalyst properties and catalytic performance [3]. Elemental analysis was carried out using JSM 5610 LV combined with INCA instrument for EDX-SEM. The total weight loss was calculated by the TGA method on the Mettler Toledo Star SW 7.01 upto 600 °C. FTIR spectra of the samples were recorded as the KBr pellet on the Perkin Elmer instrument. The spinning rate was 4–5 kHz. The BET specific surface area was calculated by using the standard Bruanuer, Emmett and Teller method on the basis of the adsorption data. Adsorption–Desorption isotherms of samples were recorded on a micromeritics ASAP 2010 surface area analyzer at −196 °C. The powder XRD pattern was obtained by using a Phillips Diffractometer (Model PW-1830). The conditions used were Cu Kα radiation (1.5417 Å).

2.1.1.4 Oxidation of Alcohols with Molecular Oxygen [4]

The catalytic activity was evaluated for oxidation of alcohols using molecular oxygen as an oxidant and *tert*-Butyl hydrogen peroxide as an initiator. Oxidation reaction was carried out in a batch type reactor operated under atmospheric pressure. In a typical reaction, measured amount of catalyst was added to a three necked flask containing alcohol at 90 °C. The reaction was started by bubbling O_2 into the liquid. The reactions were carried out by varying different parameters such as effect of % loading of PMo_{11}, reaction temperature, catalyst amount and reaction time.

After completion of the reaction, catalyst was removed and the product was extracted with dichloromethane. The product was dried with magnesium sulphate and analyzed on Gas Chromatograph (Nucon 5700 model) using BP-1 capillary column (30 m, 0.25 mm id). Product identification was done by comparison with authentic samples and finally by a combined Gas Chromatography Mass Spectrometer (Hewlett-Packard column) using HP-1 capillary column (30 m, 0.5 mm id) with EI and 70 eV ion source.

The conversion as well as selectivity was calculated on the basis of mole percent of substrates.

$$\text{Conversion}\,(\%) = \frac{(\text{initial mol}\,\%) - (\text{final mol}\,\%)}{(\text{initial mol}\,\%)}$$

$$\text{Selectivity}\,(\%) = \frac{\text{moles of product formed}}{\text{moles of substrate consumed}} \times 100$$

The turn over number (TON) was calculated using the following equation

$$\text{TON} = \frac{\text{moles of product}}{\text{moles of catalyst}}.$$

2.1.2 Result and Discussion

2.1.2.1 Characterization of Unsupported Undecamolybdophosphate

The PMo_{11} was isolated as the sodium salt after completion of the reaction and the remaining solution was filtered off. The filtrate was analyzed to estimate the amount of non reacted Mo [5]. The observed % of Mo in the filtrate was 0.5 %, which corresponds to loss of one equivalent of Mo from $H_3PMo_{12}O_{40}$. The observed values for the elemental analysis are in good agreement with the theoretical values indicating the formation of PMo_{11}. Anal. calc. (%): Na, 7.65; Mo, 50.12; P, 1.47; O, 39.52. Found (%): Na, 7.60; Mo, 49.99; P, 1.44; O, 39.92.

The TG-DTA curve of PMo_{11} is presented in Fig. 2.1. The TGA of PMo_{11} shows an initial weight loss of 16 % from 30 to 150 °C. This may be due to the removal of adsorbed water and water of crystallization. The final weight loss at around 235 °C indicates the decomposition of PMo_{11}.

DTA of PMo_{11} (Fig. 2.1) shows endothermic peaks at 80 and 140 °C, due to the loss of adsorbed water and water of crystallization respectively. In addition, DTA of PMo_{11} also shows a broad exothermic peak in the region of 270–305 °C. This may be due to the decomposition of PMo_{11}.

Number of water molecules was determined from the TGA curve using the following formula

$$18n = \frac{X(M + 18n)}{100}$$

where
n = number of water molecules
X = % loss from TGA
M = molecular weight of substance.

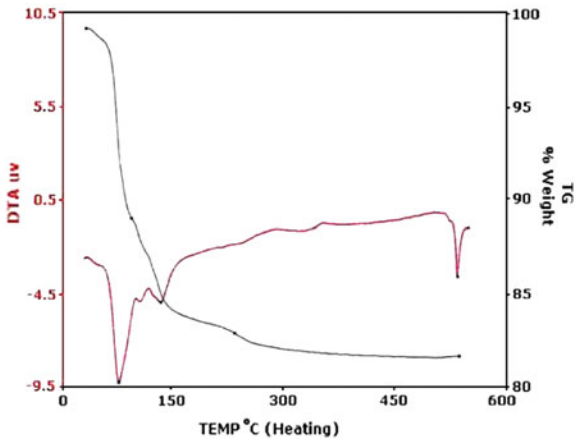

Fig. 2.1 TG-DTA of PMo_{11}

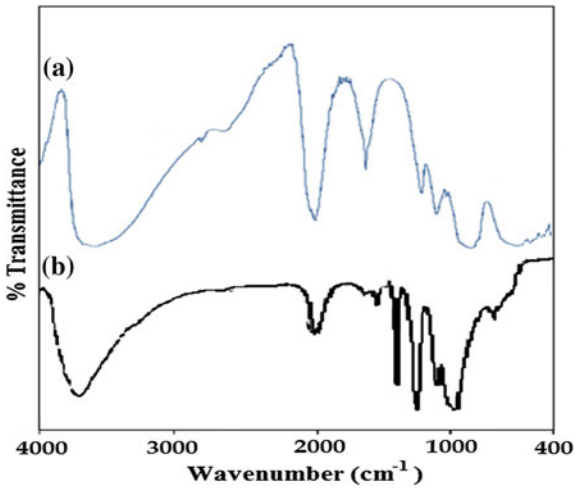

Fig. 2.2 FT-IR spectra for **a** PMo_{12} and **b** PMo_{11}

Based on studies the chemical formula of the isolated sodium salt was proposed as

$$Na_7[PMo_{11}O_{39}] \cdot 16H_2O$$

The FT-IR spectra of PMo_{12} and PMo_{11} are presented in Fig. 2.2. The bands at 1,070, 965, 870 and 790 cm^{-1} in parent Keggin PMo_{12} attributed to asymmetric stretches of P–O_a, Mo–O_t, Mo–O–Mo.

The FT-IR spectra of PMo_{11} shows P–O_a band at 1,048 and 999 cm^{-1}. Observed splitting for P–O_a band in PMo_{11} as compare to that of PMo_{12}, indicates formation of lacunary structure with Keggin unit. The FT-IR spectra of PMo_{11} also shows bands 935 and 906 cm^{-1} and 855 cm^{-1} attributed to asymmetric stretches of Mo–O_t and Mo–O–Mo, respectively and are in good agreement with reported values [6]. The shifting in the band position may be due to formation of lacuna in synthesized material.

The ^{31}P chemical shift provides important information concerning the structure, composition and electronic states of these materials. ^{31}P MAS NMR of PMo_{11} is presented in Fig. 2.3.

Van Veen [7] reported in acidic solution, phosphomolybdate was present in different type of species (e.g. $[P_2Mo_5O_{23}]^{6-}$, $[PMo_6O_{25}]^{9-}$, $[PMo_9O_{31} \cdot (OH)_3]^{6-}$, $[PMo_{10}O_{34}]^{3-}$, $[PMo_{11}O_{39}]^{7-}$ and $[PMo_{12}O_{40}]^{3-}$) in the acidified aqueous solution. The ^{31}P MAS NMR spectra shows single peak at 1.64 ppm corresponds to PMo_{11} which also indicates absence of fragmentation of PMo_{11}.

The powder X-ray pattern for PMo_{12} and PMo_{11} is represented in Fig. 2.4. The powder XRD pattern of the isolated sodium salt indicates the semi-crystalline nature of PMo_{11}. PMo_{11} shows the characteristic diffraction patterns with the typical 2θ value of 8–10° indicating the formation of lacunary molybdophosphate specie. For PMo_{11}, similar peaks with shifting as compare to that of PMo_{12} were observed indicates presence of Keggin unit.

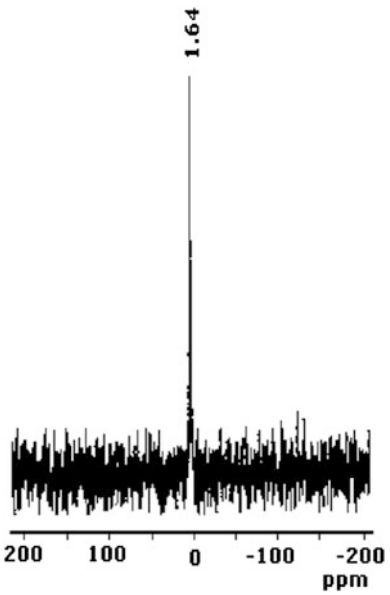

Fig. 2.3 ^{31}P MAS NMR of PMo_{11}

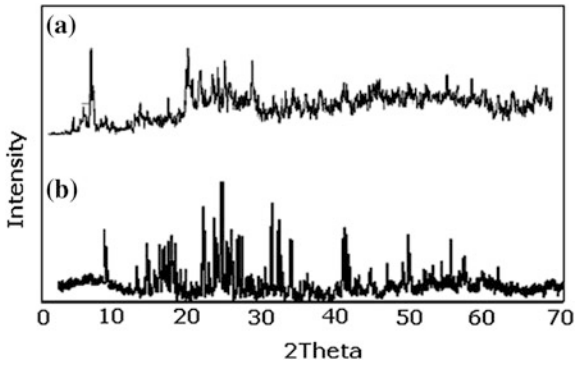

Fig. 2.4 Powder XRD pattern of **a** PMo_{12} and **b** PMo_{11}

Thus the thermal, spectral as well as diffraction studies confirms the formation of PMo_{11}.

2.1.2.2 Characterization of Undecamolybdophosphate Supported on to Metal Oxides (ZrO_2, Al_2O_3)

Any leaching of the active species from the support makes the catalyst unattractive and hence it is necessary to study the stability as well as leaching of PMo_{11} from the support. Heteropoly acids can be quantitatively characterized by the heteropoly blue colour, which is observed when it reacted with a mild reducing agent such as

ascorbic acid. In the present study, this method was used for determining the leaching of PMo_{11} from the support. Standard samples containing 1–5 % of PMo_{11} in water were prepared. To 10 mL of the above samples, 1 mL of 10 % ascorbic acid was added. The mixture was diluted to 25 mL and the resultant solution was scanned at a λmax of 785 nm for its absorbance values. A standard calibration curve was obtained by plotting values of absorbance against % concentration. 1 g of supported catalyst with 10 mL conductivity water was refluxed for 18 h. Then 1 mL of the supernatant solution was treated with 10 % ascorbic acid. Development of blue colour was not observed indicating that there was no leaching. The same procedure was repeated with benzyl alcohol and the filtrate of the reaction mixture after completion of reaction in order to check the presence of any leached PMo_{11}. The absence of blue colour indicates no leaching of PMo_{11}.

The TG-DTA data of 20 % PMo_{11}/ZrO_2 and 20 % PMo_{11}/Al_2O_3 is presented in Table 2.1.

The TGA of 20 %-PMo_{11}/ZrO_2 and 20 %-PMo_{11}/Al_2O_3 (Table 2.1) shows 17 and 5 % weight loss up to 200 °C respectively, which is due to loss of adsorbed water. Catalysts do not show any weight loss up to 300 °C, indicating the synthesized catalysts is stable up to 300 °C. DTA of 20 % PMo_{11}/ZrO_2 and 20 % PMo_{11}/Al_2O_3 show an endothermic peak in range 80–140 °C which may be due to adsorbed water. Synthesized catalysts also show a broad exothermic peak in the region 285–325 and 255–425 °C, which may be due to decomposition of PMo_{11} on the surface of the support. From the thermal study it is clearly seen that supported catalysts are stable upto 320 °C.

FT-IR was recorded to confirm the presence of reactive undegraded heteropolyanion species present on the surface of catalyst. The FT-IR data of 20 % PMo_{11}/ZrO_2 and 20 % PMo_{11}/Al_2O_3 is presented in Table 2.2. As described earlier (Fig. 2.2), FT-IR of PMo_{11} shows a band at 1,048 and 999 cm^{-1}, 935, 906 and 855 cm^{-1} attributed to asymmetric stretches of P–O, Mo–O_t and Mo–O–Mo, respectively. The synthesized catalysts retained similar bands of Keggin unit i.e. bands at 1,039, 990 and 910 cm^{-1} for 20 % PMo_{11}/ZrO_2 as well as bands at 1,052, 1,010 and 914 cm^{-1} for 20 % PMo_{11}/Al_2O_3 correspond to asymmetric stretching of P–O and Mo–O–Mo, respectively. The shifting of bands as well as the disappearance of the Mo–Ot band (935 cm^{-1}) for the supported catalysts may be due to interaction of terminal oxygen of PMo_{11} with surface hydrogen of support.

As described earlier, ^{31}P MAS NMR spectra of PMo_{11} (Fig. 2.3) show a single peak at 1.64 ppm. While, ^{31}P MAS NMR for 20 % PMo_{11}/ZrO_2 and 20 % PMo_{11}/Al_2O_3 (Fig. 2.5) reveals resonance at −2.42 and −3.47 ppm respectively.

Table 2.1 TG-DTA data PMo_{11}, 20 % PMo_{11}/ZrO_2 and 20 % PMo_{11}/Al_2O_3

Catalyst	TGA (% Weight loss up to 200 °C)	DTA (°C)	
		Endothermic	Exothermic
20 % PMo_{11}/ZrO_2	17 (continues)	80	285–325
20 % PMo_{11}/Al_2O_3	9 (continues)	80, 140	255–425

Table 2.2 FT-IR data PMo_{11}, 20 % PMo_{11}/ZrO_2 and 20 % PMo_{11}/Al_2O_3

Catalyst	FT-IR frequency (cm^{-1})		
	P–O	Mo–O_t	Mo–$O_{b,c}$–Mo
20 % PMo_{11}/ZrO_2	1,039, 990	–	910
20 % PMo_{11}/Al_2O_3	1,052, 1,010	–	914

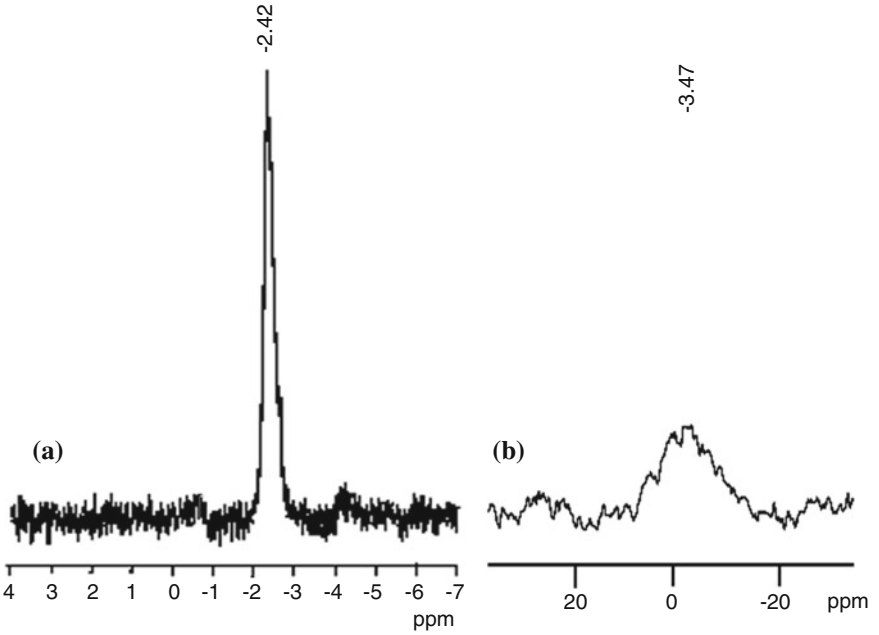

Fig. 2.5 ^{31}P MAS NMR of **a** 20 % PMo_{11}/ZrO_2 and **b** 20 % PMo_{11}/Al_2O_3

It is reported that the lower shift, i.e. deshielding, increases as the degree of adsorption and degree of fragmentation increases [8]. In the present cases, the observed chemical shift, shielding as compare to that of PMo_{11}, indicates presence of chemical interaction between PMo_{11} and supports, rather than simple adsorption. Also, a single peak for both the catalysts indicated that no fragmentation of PMo_{11} species takes place after addition to the support. Thus it can be concluded that PMo_{11} remains intact on surface of supports, after supporting on to supports.

The difference in nature of the signal as well as values of the NMR shift for 20 % PMo_{11}/ZrO_2 and 20 % PMo_{11}/Al_2O_3 may be due to the different nature of the supports. It is known that ZrO_2 is an acidic support and it has more surface hydroxyl groups as compare to that of Al_2O_3 for strong interaction through hydrogen bonding with the terminal oxygens of PMo_{11}. Thus, more shielding is observed for Al_2O_3. Thus the obtained results are in good agreement with the proposed explanation.

The values of surface area for both the series of catalysts are shown in Table 2.3. It is seen from Table 2.3 that, initially the value for surface area increases with increase in loading from 10 to 20 % while it decreases from 20 to 40 %. This may be due to the formation of multilayers of active species, PMo_{11}, onto support surface, which may cause blocking/stabilization of active sites on the monolayer.

The XRD pattern of 20 % PMo_{11}/ZrO_2 (Fig. 2.6a) and 20 % PMo_{11}/Al_2O_3 (Fig. 2.6b) shows the amorphous nature of the materials indicating that the crystallinity of the PMo_{11} is lost after supporting.

Further, it does not show any diffraction lines of lacunary PMo_{11} indicating a very high dispersion of solute as a non-crystalline form on the surface of the supports.

In order to compare the surface morphology of both the supported catalysts, the SEM pictures were taken at same magnification. The scanning electron microscopy (SEM) images of PMo_{11}, 20 % PMo_{11}/ZrO_2 and 20 % PMo_{11}/Al_2O_3 at a magnification of 100× are reported in Fig. 2.7.

Figure 2.7a shows the semi-crystalline nature of PMo_{11}. SEM images of 20 % PMo_{11}/ZrO_2 and 20 % PMo_{11}/Al_2O_3 (Fig. 2.7b, c) showed a uniform dispersion of PMo_{11} in a non-crystalline form on the surface of the support.

Table 2.3 Surface area

Catalysts	Surface area ($m^2\ g^{-1}$)
ZrO_2	170
10 % PMo_{11}/ZrO_2	191
20 % PMo_{11}/ZrO_2	197
30 % PMo_{11}/ZrO_2	188
40 % PMo_{11}/ZrO_2	187
Al_2O_3	81.0
10 % PMo_{11}/Al_2O_3	99.7
20 % PMo_{11}/Al_2O_3	101.8
30 % PMo_{11}/Al_2O_3	72.9
40 % PMo_{11}/Al_2O_3	56.2

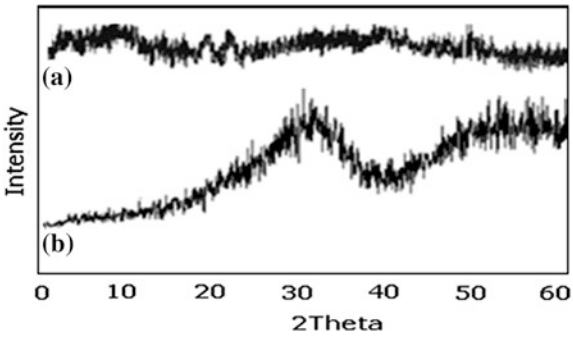

Fig. 2.6 Powder XRD pattern of **a** 20 % PMo_{11}/ZrO_2 and **b** 20 % PMo_{11}/Al_2O_3

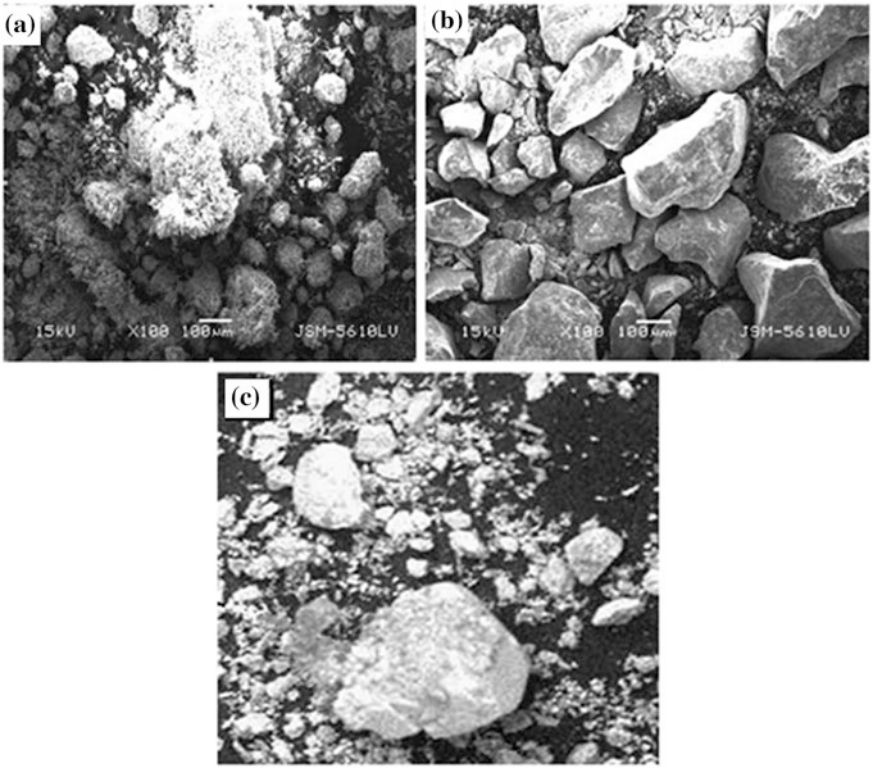

Fig. 2.7 SEM images of **a** PMo_{11} and **b** 20 % PMo_{11}/ZrO_2, **c** 20 % PMo_{11}/Al_2O_3

2.1.2.3 Catalytic Activity

A detail study was carried out on oxidation of benzyl alcohol to optimize the conditions. To ensure the catalytic activity, all reactions were carried out without catalyst and no oxidation takes place. The reaction was carried out with 25 mg of PMo_{11}/ZrO_2 and PMo_{11}/Al_2O_3 for 24 h at 90 °C. Generally, benzyl alcohol on oxidation gives benzaldehyde and benzoic acid. However, benzaldehyde was found as the major oxidation product in the present case (Scheme 2.1).

Scheme 2.1 Oxidation of benzyl alcohol

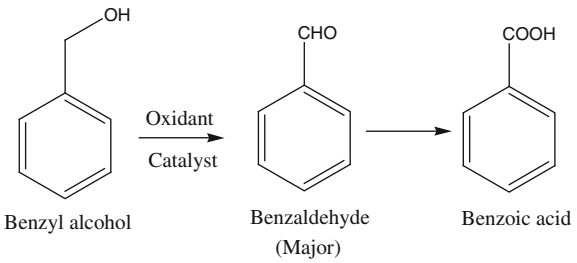

The oxidation of benzyl alcohol was carried out using 25 mg of catalysts for 24 h at 90 °C are presented in Fig. 2.8.

From Fig. 2.8 it is clear that, increase in the conversion was observed with increase in the % loading of PMo_{11} from 10 to 20 %. Further, increase in % loading from 20 to 40 %, no significant increase in conversion was observed. This may be due to at higher % loading, the particles may agglomerate on the surface, results in reduce accessibility to the active sites. Thus, loading of PMo_{11} on the supports was fixed at 20 % and detail studies were carried out over 20 % PMo_{11}/ZrO_2 and 20 % PMo_{11}/Al_2O_3.

In order to determine the optimum temperature the reaction was investigated at four different temperatures 80, 90 and 100 °C, using both the catalysts keeping other parameters fixed (amount 25 mg, time 24 h). The results for the same are presented in Fig. 2.9.

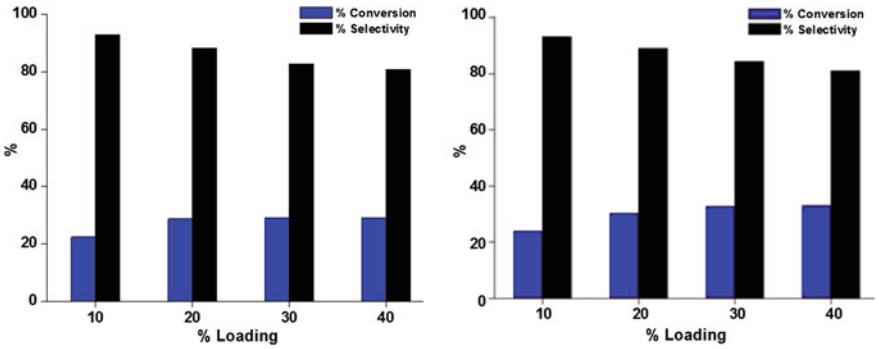

Fig. 2.8 % Conversion is based on benzyl alcohol; benzyl alcohol = 100 mmol, TBHP = 0.2 %, temp = 90 °C, time = 24 h, amount of catalyst = 25 mg, PMo_{11}/ZrO_2 (*left*) and PMo_{11}/Al_2O_3 (*right*)

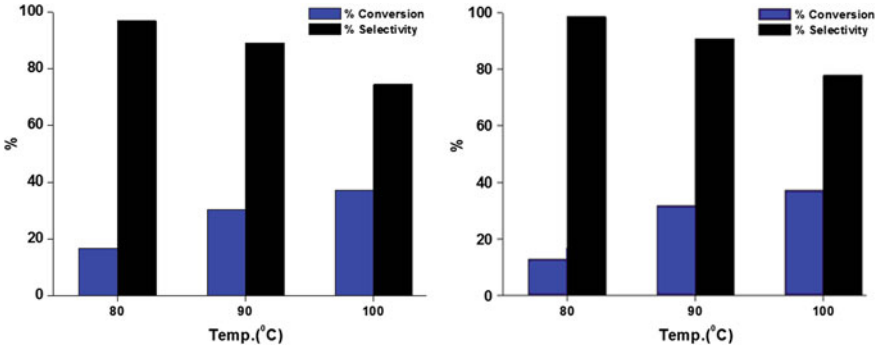

Fig. 2.9 % Conversion is based on benzyl alcohol; benzyl alcohol = 100 mmol, TBHP = 0.2 %, time = 24 h, amount of catalyst = 25 mg, PMo_{11}/ZrO_2 (*left*) and PMo_{11}/Al_2O_3 (*right*)

The results show that conversion increased with increasing temperature. At the same time, on increasing temperature from 90 to 100 °C, selectivity of benzaldehyde was decrease for both catalysts, this is due to over oxidation of benzaldehyde to benzoic acid at elevated temperature. So temperature of 90 °C was fixed for the optimum conversion of benzyl alcohol as well selectivity of desire product.

The effect of the catalyst amount on the conversion of benzyl alcohol over both the catalysts is represented in Fig. 2.10.

The catalyst amount was varied from 15 to 50 mg. It is seen from this figure that the activity increases initially up to 25 mg and then becomes constant with further increase in the amount of catalyst. However, decrease in selectivity was observed. In the present case, water is formed as a by-product which is polar in nature. In presence of polar molecules, heteropolyacids exhibit pseudoliquid behaviour [9] in which catalytic activity is directly proportional to the active amount of the catalyst. So the same observation is expected in case of LPOMs. Further, increase in the amount blocks/stabilizes the active sites. Hence, no change in conversion is expected. The obtained results are in good agreement with the proposed explanation.

The effect of reaction time is shown in Fig. 2.11. It is seen from figure that initially with increase in reaction time, the conversion also increases. After some time, the conversion attains stability. This may be due to the fact that the activation of the catalyst as well as the attainment of equilibrium requires time.

Once the equilibrium is attained, the conversion becomes almost constant. But at the same time, selectivity of benzaldehyde decreases. This may be due to over oxidation of benzaldehyde to benzoic acid. Thus, reaction time at 24 h was optimized for optimum conversion of benzyl alcohol as well selectivity of benzaldehyde.

The optimum conditions for 23.7 % conversion with 92.3 % selectivity for benzaldehyde with 20 %-PMo_{11}/ZrO_2 and 22.5 % conversion with 94.8 % selectivity for benzaldehyde with 20 %-PMo_{11}/Al_2O_3 are, catalyst amount = 25 mg, temperature = 90 °C, time = 24 h.

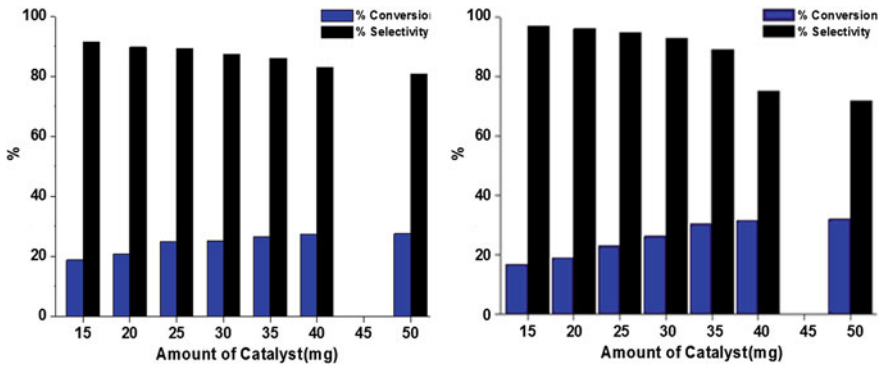

Fig. 2.10 % Conversion is based on benzyl alcohol; benzyl alcohol = 100 mmol, TBHP = 0.2 %, temp = 90 °C, time = 24 h, PMo_{11}/ZrO_2 (*left*) and PMo_{11}/Al_2O_3 (*right*)

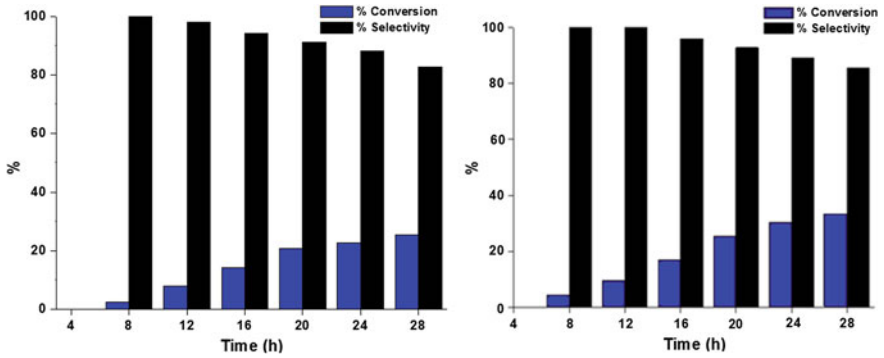

Fig. 2.11 % Conversion is based on benzyl alcohol; benzyl alcohol = 100 mmol, TBHP = 0.2 %, temp = 90 °C, amount of catalyst = 25 mg, PMo_{11}/ZrO_2 (*left*) and PMo_{11}/Al_2O_3 (*right*)

In order to see scope and limitations of present catalytic systems, oxidation of various alcohols was carried out with supported catalysts under optimized conditions and results are shown in Table 2.4. It was observed from Table 2.4 that, oxidation of secondary alcohol is easier as compare to primary alcohols.

The observed trend is in good agreement with reported in art [10]. In all cases, very high TON is observed. It is known that, oxidation of long chain alcohols (C_8 and onwards) is still challenging task because of lower reactivity [11] and thus present catalytic system is also not applicable to less reactive long chain primary alcohol such as 1-octanol. For the present catalytic system, the reactivity of the alcohols was found in the order primary < cyclic secondary < aromatic.

Table 2.4 Oxidation of various alcohols with O_2, under optimized conditions

Alcohols	Conversion (%)	Products	Selectivity (%)	TON
[a]Benzyl alcohol	23.7	Benzaldehyde	92.3	11,814
		Benzoic acid	7.7	
[a]Cyclopentanol	22.7	Cyclopentanone	>99	11,609
[a]Cyclohexanol	22.4	Cyclohexanone	>99	11,456
[a]1-Hexanol	9.1	1-Hexanal	>99	4,654
[a]1-Octanol	–	–	–	–
[b]Benzyl alcohol	22.5	Benzaldehyde	94.8	11,216
		Benzoic acid	5.2	
[b]Cyclopentanol	22.2	Cyclopentanone	>99	11,353
[b]Cyclohexanol	21.6	Cyclohexanone	>99	11,046
[b]1-Hexanol	8.2	1-Hexanal	>99	4,194
[b]1-Octanol	–	–	–	–

% Conversion is based on alcohol; alcohol = 100 mmol, TBHP = 0.2 %, temp = 90 °C, time = 24 h, amount of catalyst = 25 mg

[a] $(PMo_{11})_2/ZrO_2$

[b] $(PMo_{11})_2/Al_2O_3$

It is well know that support does not play always merely a mechanical role but it can also modify the catalytic properties of the catalysts. So, in order to see the effect of support, comparison of activity of 20 % PMo_{11}/ZrO_2 and 20 % PMo_{11}/Al_2O_3 was done for oxidation of benzyl alcohol under optimized conditions and results are presented in Table 2.4. Generally, oxidation of benzyl alcohol gives benzaldehyde (major), with over oxidation product benzoic acid (minor). These types of over oxidation reactions are directly promoted by acidity of the catalyst. So, observed result i.e. lower selectivity of benzaldehyde in case of PMo_{11}/ZrO_2 is attributed to acidity of ZrO_2.

2.1.2.4 Heterogeneity Test

Heterogeneity test was carried out for the oxidation of benzyl alcohol (Fig. 2.12) over PMo_{11}/ZrO_2 as examples.

For the rigorous proof of heterogeneity, a test [12] was carried out by filtering catalyst from the reaction mixture at 90 °C after 16 h and the filtrate was allowed to react up to 24 h. Reaction mixture of 16 h and the filtrate were analyzed by gas chromatography. Similar test was carried for PMo_{11}/Al_2O_3. No change in the % conversion as well as % selectivity was found indicating the present catalysts fall into category C [12] i.e., active species does not leach and the observed catalysis is truly heterogeneous in nature.

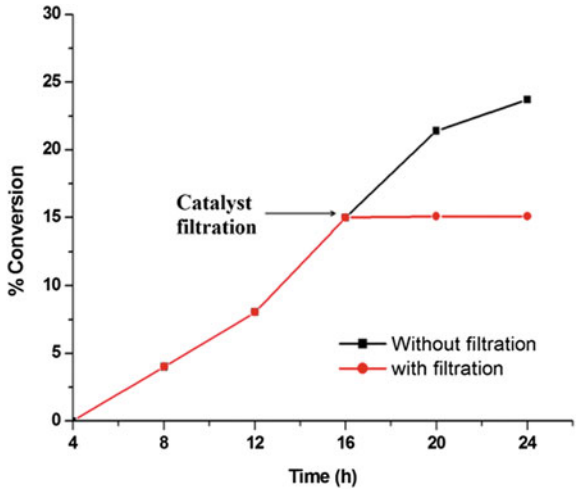

Fig. 2.12 % Conversion is based on benzyl alcohol; benzyl alcohol = 100 mmol, O_2, TBHP = 0.2 %, amount of 20 % PMo_{11}/ZrO_2 = 25 mg; temperature 90 °C

Table 2.5 Oxidation of benzyl alcohol with fresh and regenerated catalysts

Cycle	Conversion (%)	Selectivity (%)
		Benzaldehyde
Fresh	23.1[a]/23.0[b]	92.3[a]/94.6[b]
1	22.9[a]/22.9[b]	92.2[a]/95.0[b]
2	22.9[a]/22.9[b]	92.2[a]/94.9[b]
3	22.9[a]/22.5[b]	92.0[a]/94.2[b]
4	22.7[a]/22.6[b]	92.0[a]/94.2[b]

% Conversion is based on benzyl alcohol; benzyl alcohol = 100 mmol, TBHP = 0.2 %, temp = 90 °C, time = 24 h, amount of catalyst = 25 mg

[a] 20 % PMo_{11}/ZrO_2

[b] 20 % PMo_{11}/Al_2O_3

2.1.2.5 Catalytic Activity of Regenerated Catalysts

The catalyst was recycled in order to test for its activity as well as its stability. The catalysts remain insoluble under the present reaction conditions. The leaching of Mo from catalyst support was confirmed by carrying out an analysis of the used catalyst (EDS) as well as the product mixtures (AAS). The analysis of the used catalyst did not show an appreciable loss in the Mo content as compared to the fresh catalyst. The analysis of the product mixtures showed that if any Mo was present it was there in an amount below the detection limit, which corresponded to less than 1 ppm. These observations strongly suggest that the present catalyst is truly heterogeneous in nature.

Catalysts were separated easily by simple filtration followed by washing with dichloromethane and dried at 100 °C. Oxidation reaction was carried out with the regenerated catalysts, under the optimized conditions. The data for the catalytic activity is represented in Table 2.5. It is seen from the table that there was no change in selectivity, however, a little decrease in conversion was observed. This shows that the catalysts are stable, regenerated and reused successfully up to 4 cycles.

2.1.2.6 Characterization of Regenerated Catalysts

20 % PMo_{11}/ZrO_2 and 20 % PMo_{11}/Al_2O_3 were regenerated and characterized for FT-IR in order to confirm the retention of the catalyst structure, after the completion of the reaction. The FT-IR data for the fresh as well as the regenerated catalysts are represented in Fig. 2.13. No appreciable shift in the FT-IR band position of the regenerated catalyst indicates the retention of Keggin type PMo_{11} onto supports.

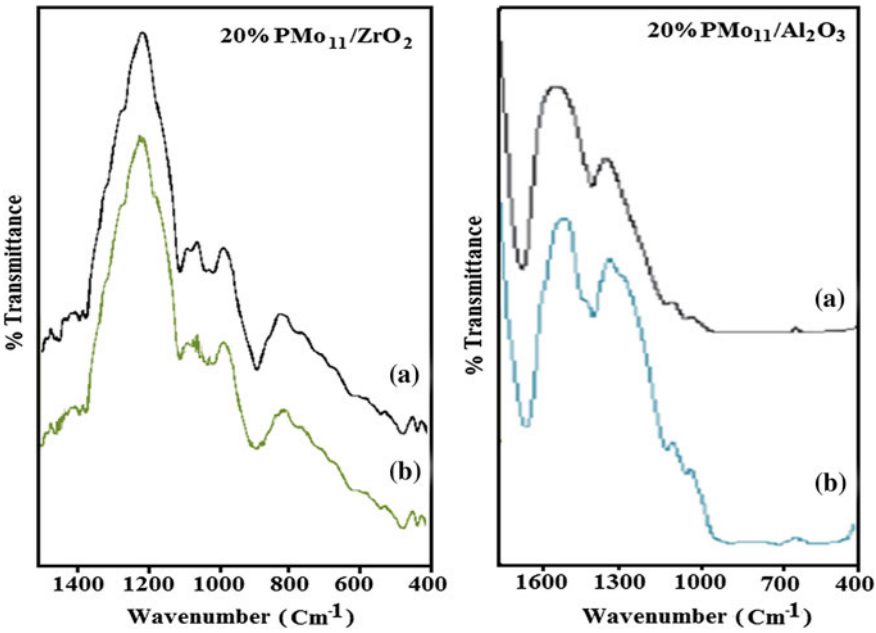

Fig. 2.13 FT-IR spectra of **a** fresh and **b** recycled (fourth cycle) catalysts

2.2 Undecamolybdophosphate Anchored to Porous Supports (Zeolite Hβ, MCM-41)

2.2.1 Experimental

2.2.1.1 Materials

All the chemicals used were of A. R. grade. CTAB (cetyltrimethyl ammonium bromide), TEOS (tetraethyl orthosilicate), benzyl alcohol, cyclopentanol, cyclohexanol, 1-hexanol, 1-octanol, 70 % aq. TBHP, NaOH and dichloromethane were obtained from Merck and used as received. The sodium form of zeolite β (Naβ) with Si/Al ratio 10 was purchased from Zeolites and Allied Products, Bombay, India, and used as received.

2.2.1.2 Synthesis of the Supports (MCM-41, Hβ) [13]

CTAB was added to a very dilute solution of NaOH with stirring at 60 °C. When the solution became homogeneous, TEOS was added dropwise, and the obtained gel was aged for 2 h. The resulting product was filtered, washed with distilled

water, and then dried at room temperature. The obtained material was calcined at 555 °C in air for 5 h and designated as MCM-41.

Treatment of the Support (zeolite-Hβ)
Naβ was converted in to the NH_4^+ form by conventional ion exchange method [14] using a 10 wt%, 1 M NH_4Cl aqueous solution. The resulting NH_4^+ type zeolite was further converted to H^+ type by calcination in air at 550 °C for 6 h.

2.2.1.3 Synthesis of Supported Catalysts [15]

Supporting of PMo_{11} to MCM-41 and Hβ
A series of catalysts containing 10–40 % of PMo_{11} supported to support (MCM-41 and Hβ) were synthesized by impregnation method. One gram of support was impregnated with an aqueous solution of PMo_{11} (0.1/10–0.4/40 g/mL of double distilled water) and dried at 100 °C for 10 h. The obtained materials were designated as 10 % PMo_{11}/MCM-41, 20 % PMo_{11}/MCM-41, 30 % PMo_{11}/MCM-41, and 40 % PMo_{11}/MCM-41, respectively, as well as 10 % PMo_{11}/Hβ, 20 % PMo_{11}/Hβ, 30 % PMo_{11}/Hβ, and 40 % PMo_{11}/Hβ, respectively.

Characterization specifications and catalytic reaction is similar as mentioned in Sects. 2.1.1.3 and 2.1.1.4.

2.2.2 Result and Discussion

2.2.2.1 Characterization of Undecamolybdophosphate Anchored to Porous Supports (Zeolite-Hβ, MCM-41)

TGA curves of zeolite support and catalysts are shown in Fig. 2.14. The TGA of PMo_{11} (Fig. 2.14a) shows the initial weight loss of 16 % from 30 to 200 °C. This may be due to the removal of adsorbed water molecules. The final weight loss of 1.8 % at around 275 °C indicates the loss of water of crystallisation. A unique weight loss of 13–15 % was observed up to 250 °C for zeolite support (Fig. 2.14b), which is attributed to desorption of physically adsorbed water. No further weight loss was observed beyond 250 °C which indicates zeolite Hβ retains its framework structure up to 600 °C. TGA of MCM-41 (Fig. 2.14c) shows initial weight loss of 6.14 % at 100 °C. This may be due to the loss of adsorbed water molecules. The final 7.92 % weight loss above 450 °C may be due to the condensation of silanol groups to form siloxane bonds. After that, the absence of any weight loss indicates that support is stable up to 550 °C. The TGA of 30 % PMo_{11}/Hβ (Fig. 2.14d) shows initial weight loss of 11.2 % up to 150 °C which may be due to the removal of adsorbed water molecules. No significant weight loss occurs up to 350 °C (2.6 %), which indicates the stability of the catalyst up to 350 °C. The removal of the Mo–O moiety from the parent PMo_{12} leads to the thermally less stable material PMo_{11}.

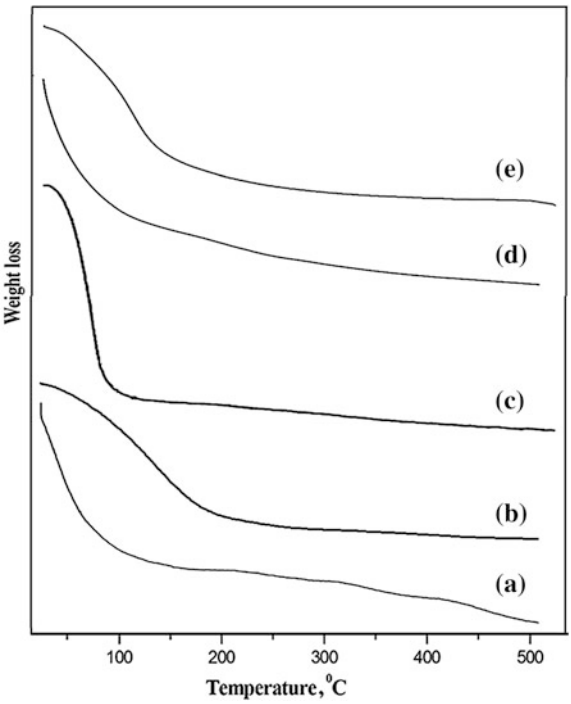

Fig. 2.14 TGA curves of **a** PMo_{11}, **b** Hβ, **c** MCM-41, **d** 30 % PMo_{11}/Hβ, and **e** 30 % PMo_{11}/MCM-41

The thermal stability values of PMo_{11} and supported PMo_{11} are 305 and 350 °C respectively. The TGA of 30 % PMo_{11}/MCM-41 (Fig. 2.14e) shows initial weight loss up to 150 °C may be due to the removal of adsorbed water molecules. No significant loss occurs up to 350 °C, which indicates the stability of the catalyst up to 350 °C.

The FT-IR spectra of MCM-41, Hβ, PMo_{11} and 30 % PMo_{11}/Hβ and 30 % PMo_{11}/MCM-41 are presented in Fig. 2.15. The FT-IR spectrum of MCM-41 (Fig. 2.15b) shows a broad band around 1,300–1,000 cm^{-1} corresponding to ν_{as} (Si–O–Si). The bands at 801 and 458 cm^{-1} are due to symmetric stretching and bending vibration of Si–O–Si, respectively. The band at 966 cm^{-1} corresponds to ν_s (Si–OH). The bands at 1048 and 999 cm^{-1}, 935 and 906 cm^{-1} and 855 cm^{-1} in parent PMo_{11} (Fig. 2.15a) are attributed to asymmetric stretching of P–O, Mo–Ot and Mo–O–Mo respectively. The spectrum of 30 % PMo_{11}/MCM-41 (Fig. 2.15c) shows bands at 965 and 918 cm^{-1} assigned to P–O and Mo = O stretches, respectively. The shift in the bands is an indication of strong chemical interaction between PMo_{11} and the silanol groups of MCM-41.

The FT-IR spectra for Hβ and 30 % PMo_{11}/Hβ (Fig. 2.15) shows large and broad peak appearing in range 1,060–1,090 cm^{-1} due to asymmetric stretching vibration O–T–O (ν_{asym}), which is sensitive to the silicon and aluminum contents in the zeolite framework. A band at 455 cm^{-1} is characteristic of the pore opening. The shifting and broadening of bands as well as disappearance of Mo–Ot band

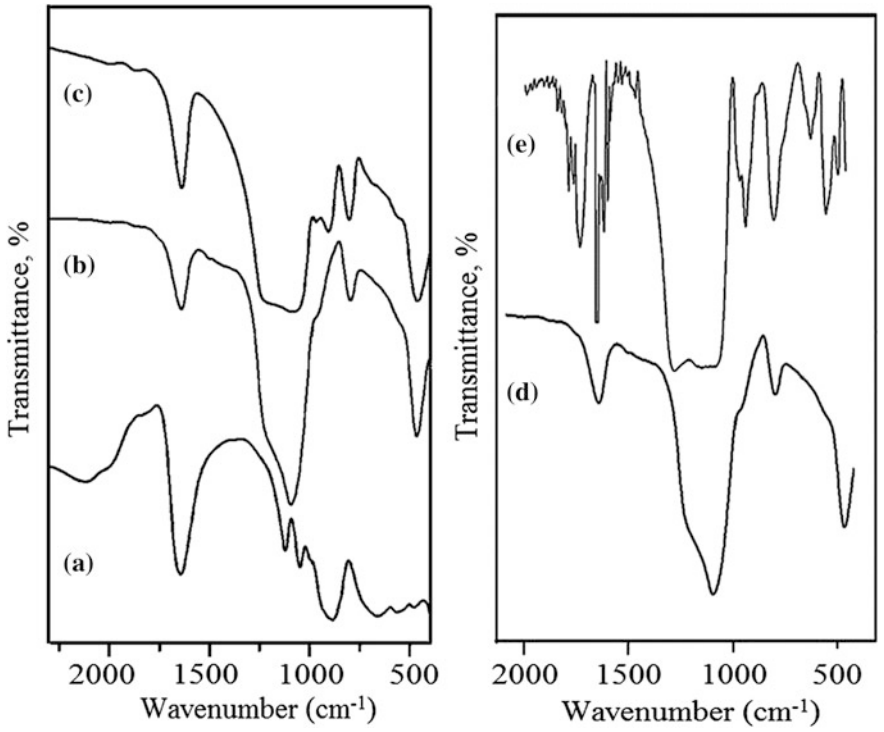

Fig. 2.15 FT-IR of **a** PMo_{11}, **b** MCM-41, **c** 30 % PMo_{11}/MCM-41, **d** Hβ and **e** 30 % PMo_{11}/Hβ

(935 cm^{-1}) may be due to strong chemical interaction of terminal oxygen of PMo_{11} with Hβ, which was further confirmed by FT-Raman analysis.

FT-Raman spectra of PMo_{11} and both the catalysts are displayed in Fig. 2.16. The FT-Raman spectrum of PMo_{11} shows typical bands at 947 (ν_s(Mo–O_d)), 932 (ν_{as}(Mo–O_d)), 891 and 550 (ν_{as}(Mo–Ob–Mo)), 355 (ν_{as}(O_a–P–O_a)) and 217 (ν_s(Mo–O_a)), where O_a, O_b, O_c, and O_d are attributed to the oxygen atoms connected to phosphorus, to oxygen atoms bridging two molybdenums (from two different triads for O_b and from the same triad for O_c), and to the terminal oxygen Mo = O, respectively. The FT-Raman spectrum of 30 % PMo_{11}/MCM-41 shows the retention of all the characteristic bands at 916 (ν_s(Mo–O_d)), 876 (ν_{as}(Mo–O_d)), 793 and 548 (ν_{as}(Mo–O_b–Mo)), 323 (ν_{as}(O_a–P–O_a)) and 140 (νs(Mo–O_a)), which indicates that the structure of PMo_{11} has been retained after anchoring to the support. The FT-Raman spectrum of 30 % PMo_{11}/Hβ (Fig. 2.16) shows the retention of all the characteristic bands of PMo_{11} which indicates that the structure of PMo_{11} has been retained after anchoring to the support. However, a large shift was observed for all characteristic bands indicating the presence of very strong interaction between the oxygen of PMo_{11} and Hβ.

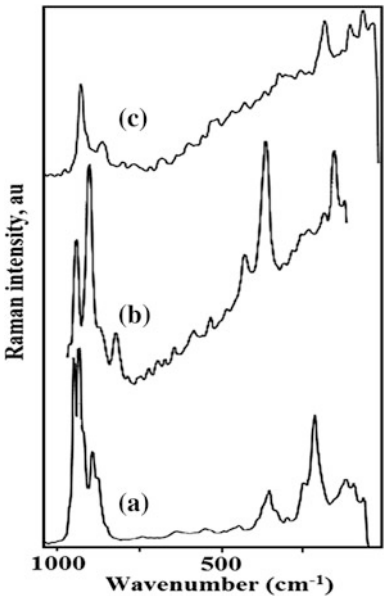

Fig. 2.16 FT-Raman spectra of **a** PMo_{11}, **b** 30 % PMo_{11}/MCM-41, and **c** 30 % PMo_{11}/Hβ

The decrease in the specific surface area for 30 % PMo_{11}/MCM-41 (485 m^2 g^{-1}) as compared to that of MCM-41 (659 m^2 g^{-1}) is as expected and is the first indication of chemical interaction between available surface oxygen of PMo_{11} and the proton of the silanol group of MCM-41. Figure 2.17 shows the nitrogen adsorption–desorption isotherms and BET pore size distribution curves for Hβ and 30 % PMo_{11}/Hβ. Both Specific surface area and pore diameter strongly decreased for PMo_{11}-containing Hβ relative to the starting support. The decrease in the specific surface area for 30 % PMo_{11}/Hβ (362 m^2 g^{-1}) as compared to that of Hβ (587.2 m^2 g^{-1}) is as expected and is the first indication of chemical interaction between available surface oxygen of PMo_{11} and Hβ. The nitrogen adsorption

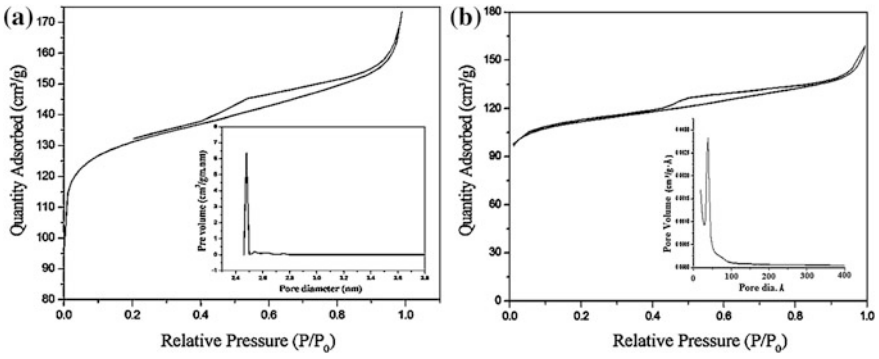

Fig. 2.17 Nitrogen sorption and pore size distribution of **a** Hβ and **b** 30 % PMo_{11}/Hβ

isotherms of support and catalyst are displayed in Fig. 2.17. Both samples showed Type (IV) pattern with three stages: monolayer adsorption of nitrogen on the walls of mesopores (P/Po < 0.4), the part characterized by a steep increase in adsorption due to capillary condensation in mesopores with hysteresis (P/Po = 0.4–0.8), and multilayer adsorption on the outer surface of the particles. It was observed that pore diameter was decreased after anchoring PMo_{11} on to the support.

The FT-IR, FT-Raman, BET shows that PMo_{11} remains intact even after anchoring and there exists a strong chemical interaction of PMo_{11} with the support.

2.2.2.2 Catalytic Activity

In the present work, a detailed catalytic study was carried out over 30 % PMo_{11}/Hβ for the oxidation of benzyl alcohol by varying different parameters like % loading, catalyst amount, reaction time and temperature to optimize the conditions for the maximum conversion.

Figure 2.18 shows the effect of % loading of PMo_{11} on the oxidation of benzyl alcohol using molecular oxygen. The conversion increases with increase in the % loading of PMo_{11} from 10 to 20 %. There is a drastic increase in the conversion on increasing loading from 20 to 30 %. The conversion reaches 25.5 % for 30 % loaded catalyst and further increase in the loading to 40 % does not affect the conversion significantly. This is because, at higher % loading, the active species agglomerate on the surface of the support resulting in low accessibility to the active sites. It is also seen that at higher loading the selectivity for benzaldehyde decreases. Hence, 30 % loading was selected for further study.

The amount of catalyst has a significant effect on the oxidation of benzyl alcohol. Reaction was carried out by taking catalyst amount in the range 15–30 mg (Fig. 2.19). Initially, on increasing catalyst amount from 10 to 25 mg, the conversion increases sharply. Further increase in the catalyst amount does not increase

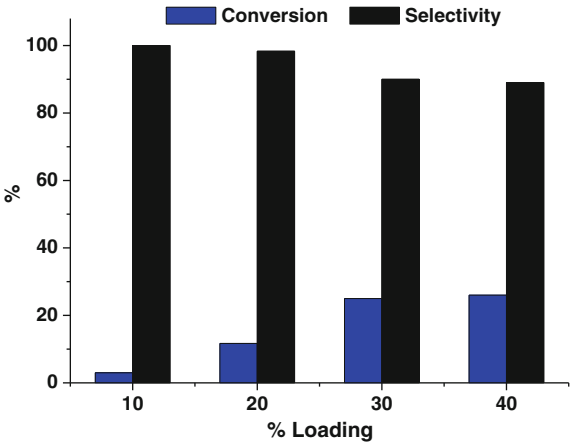

Fig. 2.18 % Conversion is based on benzyl alcohol; benzyl alcohol = 100 mmol, TBHP = 0.2 mmol, amount of catalyst = 25 mg, time = 24 h, temp = 90 °C

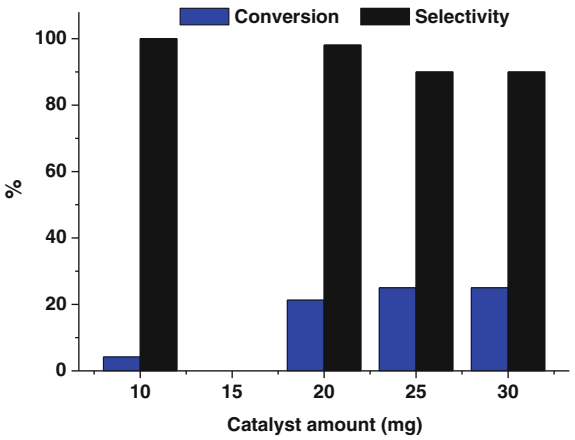

Fig. 2.19 % Conversion is based on benzyl alcohol; benzyl alcohol = 100 mmol, TBHP = 0.2 mmol, time = 24 h, temp = 90 °C

the conversion very significantly. Therefore, 25 mg amount of catalyst has been considered as optimum for the maximum conversion.

The effect of reaction time on the selective oxidation was carried out by monitoring % conversion at different time intervals. It is seen from Fig. 2.20 that with increase in reaction time, the % conversion also increases. Initial conversion of benzyl alcohol increased with the reaction time. This is due to the reason that more time is required for the formation of reactive intermediate (substrate + catalyst) which finally converts into the products. It was seen that 25.5 % conversion was observed at 24 h; when the reaction was allowed to continue for 25 h, no significant conversion was observed, but selectivity of benzaldehyde decreases. The maximum conversion was achieved at 24 h of reaction time.

The effect of temperature on the oxidation of benzyl alcohol was investigated by varying temperature in the range of 70–100 °C (Fig. 2.21). An optimum of 25.5 %

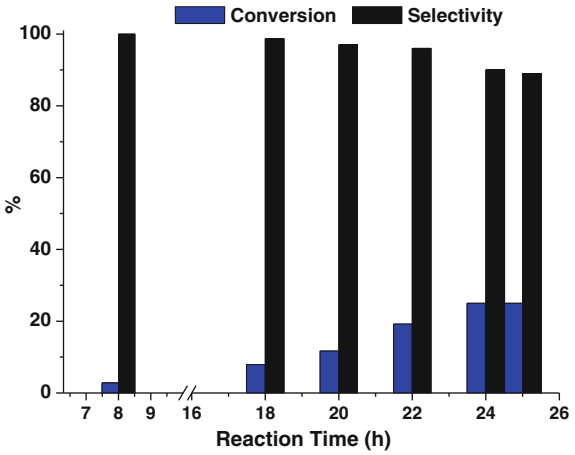

Fig. 2.20 % Conversion is based on benzyl alcohol; benzyl alcohol = 100 mmol, TBHP = 0.2 mmol, amount of catalyst = 25 mg, time = 24 h, temp = 90 °C

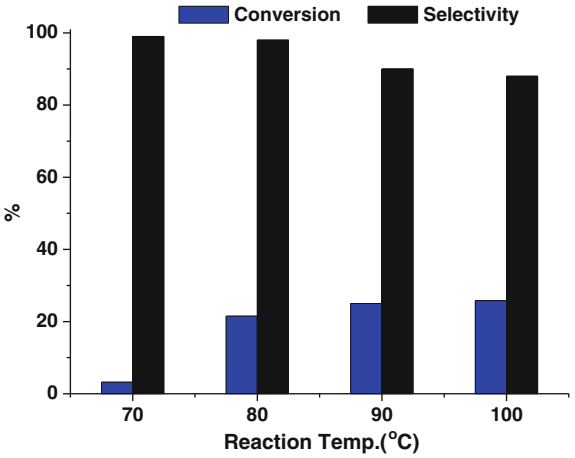

Fig. 2.21 % Conversion is based on benzyl alcohol; benzyl alcohol = 100 mmol, TBHP = 0.2 mmol, amount of catalyst = 25 mg, time = 24 h

conversion was achieved at 90 °C temperature. When temperature was increased further to 100 °C there is no significant increase in conversion. This is due to over-oxidation of benzaldehyde to benzoic acid at elevated temperature. Hence, 90 °C was considered as optimum for the maximum conversion as well as selectivity.

The optimum conditions for maximum % conversion (25.5 %) of benzyl alcohol to benzaldehyde over 30 % PMo_{11}/Hβ are: loading of PMo_{11} = 30 %, amount of catalyst = 25 mg (0.227 wt%), time = 24 h, temperature = 90 °C. Under the same conditions the maximum % conversion over 30 % PMo_{11}/MCM-41 was found to be 28 %.

The control experiments with Hβ and PMo_{11} were also carried out under optimized conditions (Table 2.6). It can be seen from Table 2.6 that the supports are inactive towards the oxidation of benzyl alcohol indicating the catalytic activity is only due to PMo_{11}. The same reaction was carried out by taking the active amount of PMo_{11} (5.7 mg). It was found that the active catalyst gives 25.2 % conversion of benzyl alcohol with 91 % selectivity towards benzaldehyde. Similar obtained activity for supported catalysts indicate that PMo_{11} is the real active species. Thus, we are successful in supporting PMo_{11} onto MCM-41 as well as Hβ without any significant loss in activity and hence in overcoming the traditional problems of homogeneous catalysis.

Table 2.6 Control experiments over the catalyst and the support

Catalyst	Conversion %	Selectivity %
Hβ	<1	100
MCM-41	<1	100
30 % PMo_{11}/MCM-41	28.0	90
PMo_{11}	25.2	91
30 % PMo_{11}/Hβ	25.5	90

% conversion is based on benzyl alcohol; amount of PMo_{11} = 5.7 mg, amount of Hβ = 19.3 mg, time = 24 h, temp = 90 °C

Table 2.7 Oxidation of various alcohols over supported catalysts, under optimized conditions

Substrate	% Conversion	Products (% selectivity)	TON
[a]Benzyl alcohol	25.5	Benzaldehyde (90)	9,551
[a]Cyclohexanol	21	Cyclohexanone (>99)	8,580
[a]Cyclopentanol	20	Cyclopentanone (>99)	8,171
[a]1-Hexanol	9	1-hexanal (>99)	3,745
[a]1-Octanol	NC	1-Octanal (–)	–
[b]Benzyl alcohol	28	Benzaldehyde (90)	10,487
[b]Cyclohexanol	22	Cyclohexanone (>99)	8,989
[b]Cyclopentanol	20	Cyclopentanone (>99)	8,240
[b]1-Hexanol	15	1-hexanal (>99)	5,618
[b]1-Octanol	NC	1-Octanal (–)	–

% Conversion is based on benzyl alcohol; reactions of alcohols with O_2: TBHP = 0.2 mmol, amount of catalyst = 25 mg, temp = 90 °C, time = 24 h

[a] 30 % PMo_{11}/Hβ

[b] 30 % PMo_{11}/MCM-41

In order to explore the applicability of the method for a selective aerobic oxidation different alcohol substrates were studied (Table 2.7). Employing this system, benzylic, primary and secondary alcohols were oxidized to ketones or aldehydes at 90 °C with moderate to good conversions and excellent selectivity. It was observed from Table 2.7 that oxidation of secondary alcohol was easier as compared to primary alcohols. Also, it was observed that the long chain primary alcohol is very less reactive under the present reaction conditions. In all the cases we were able to achieve excellent TON for all the alcohols.

As described earlier, type of support does not play always merely a mechanical role but it can also modify the catalytic property of the catalysts. The difference in catalytic activity and product selectivity in oxidation reaction of benzyl alcohol may be due to the nature of supports such as structural mesoporosity and high specific surface area. Hence, the obtained results of 30 % PMo_{11}/Hβ were compared with 30 % PMo_{11}/MCM-41. From Table 2.7 it is seen that benzyl alcohol conversion is higher in the case of 30 % PMo_{11}/MCM-41. This might be due to difference in the surface area of the catalysts where surface area of 30 % PMo_{11}/MCM-41(485 $m^2\ g^{-1}$) is higher compared to 30 % PMo_{11}/Hβ (362 $m^2\ g^{-1}$). It is well known that the products distribution is affected by acidity of the catalyst. Generally, oxidation of benzyl alcohol gives benzaldehyde (major), with over oxidation product benzoic acid (minor). These types of over oxidation reactions are directly promoted by acidity of the catalyst. So, observed result i.e. lower selectivity (90 %) of benzaldehyde for both the catalysts is attributed to acidity of the support, as it is well known that MCM-41 and zeolite Hβ both exhibit acidity. Hence the order of catalytic activity observed was 30 % PMo_{11}/MCM-41 > 30 % PMo_{11}/Hβ.

2.2.2.3 Heterogeneity Test

Heterogeneity test [12] was carried out for the oxidation of benzyl alcohol (Table 2.8). For the rigorous proof of heterogeneity, test was carried out by filtering catalyst from the reaction mixture at 90 °C after 18 h and the filtrate was allowed to react up to 24 h. The reaction mixture of 18 h and the filtrate were analysed by gas chromatography. No change in the % conversion as well as % selectivity was found indicating the present catalysts fall into category C i.e., active species does not leach and the observed catalysis is truly heterogeneous in nature. It also confirms that the reactions are not just auto-oxidation but the catalyst plays an important role for selective conversion of the substrates.

2.2.2.4 Catalytic Activity of Regenerated Catalysts

Oxidation of benzyl alcohol was carried out with the recycled supported catalysts, under the optimized conditions. The catalysts were removed from the reaction mixture after completion of the reaction by simple centrifugation; the first washing was given with dichloromethane to remove the products, then the subsequent washings were done by double distilled water and then dried at 100 °C, and the recovered catalyst was charged for the further run. No appreciable decrease in the conversion was observed up to two cycles (Table 2.9). The reused catalyst was further characterized by FT-IR and EDX analysis.

2.2.2.5 Characterization of Regenerated Catalysts

EDX elemental analysis performed on the recycled and fresh catalyst (Fresh: P = 0.37 %, Mo = 12.0 %; recycled: P = 0.33 %, Mo = 11.3 %) shows that the all elements in the recycled catalysts are retained. The FT-IR data for the fresh as well as the recycled catalysts are presented in Fig. 2.22. The FT-IR of recycled 30 % PMo_{11}/MCM-41 shows bands at 965 and 918 cm^{-1} assigned to P–O and Mo=O stretches, respectively. Similar observations can be made for recycled 30 % PMo_{11}/

Table 2.8 Heterogeneity test

Catalyst	Conversion %	Selectivity %
30 % PMo_{11}/Hβ (18 h)	8	98
Filtrate (24 h)	8	98
30 % PMo_{11}/MCM-41 (16 h)	12	98
Filtrate (24 h)	12	97

% Conversion is based on benzyl alcohol; amount of catalyst = 25 mg; temperature = 90 °C

Table 2.9 Recycling studies under the optimised conditions

Cycle[a,b]	Conversion (%)[a,b]	Selectivity (%)[a,b]	TON[a,b]
Fresh	28, 25.5	90, 90	10,487, 9,551
1	26, 25.0	89, 89	9,738, 9,364
2	25, 24.6	89, 87	9,363, 9,214

% Conversion is based on benzyl alcohol; Benzyl alcohol, O_2: 0.2 mmol TBHP, temp, 90 °C, time, 24 h, catalyst amount 25 mg

[a] 30 % PMo_{11}/MCM-41

[b] 30 % PMo_{11}/Hβ

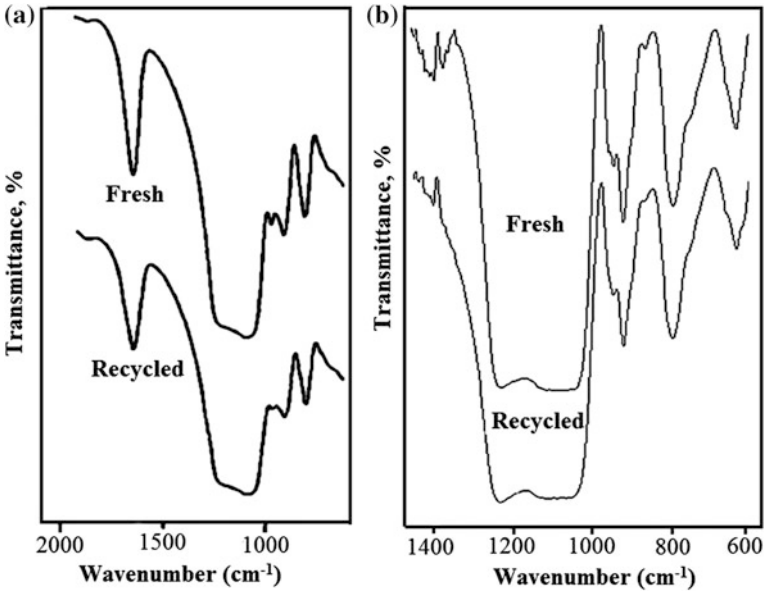

Fig. 2.22 FT-IR spectra of regenerated catalysts **a** 30 % PMo_{11}/MCM-41 and **b** 30 % PMo_{11}/Hβ

Hβ where almost all the bands are observed for PMo_{11}. No appreciable shift in the FT-IR band position of the regenerated catalyst compared to fresh 30 % PMo_{11}/Hβ indicates the retention of structure of PMo_{11} in the catalyst.

References

1. Pathan S, Patel A (2011) Dalton Trans 40:348–355
2. Patel A, Pathan S (2012) Ind Eng Chem Res 51(2):732–740
3. Richards R (ed) (2006) Surface and nanomolecular catalysis (Chap. 1). CRC Press, Taylor and Francis
4. Pathan S, Patel A (2014) Chem Eng J 243C:183–191

5. Vogel A (1951) A textbook of quantitative inorganic analysis, 2nd edn. Longmans, Green and Co., London
6. Okuhara T, Mizuno N, Misono M (1996) Adv Catal 41:113–252
7. Van Veen JAR, Sundmeijer O, Emeis CA, De Wit HJ (1986) J Chem Soc Dalton Trans 9:1825–1831
8. Edwards JC, Thiel CY, Benac B, Knifton JF (1998) Catal Lett 51:77–83
9. Shanmugam S, Viswanathan B, Varadarajan TK (2004) J Mol Catal A Chem 223:143–147
10. Balogh-Hergovicha E, Speier G (2005) J Mol Catal A Chem 230:79–83
11. Dhakshinamoorthy A, Alvaro M, Garcia H (2011) ACS Catal 1:48–53
12. Sheldon A, Walau M, Arends IWCE, Schuchurdt U (1998) Acc Chem Res 31:485–493
13. Cai Q, Luo ZS, Pang WQ, Fan YW, Chen XH, Cui FZ (2001) Chem Mater 13:258–263
14. Chidambaram M, Venkatesan C, Moreaub P, Finiels A, Ramaswamy AV, Singh AP (2002) Appl Catal A Gen 224:129–140
15. Narkhede N, Patel A, Singh S (2014) Dalton Trans 43:2512–2520

http://www.springer.com/978-3-319-12987-7

Polyoxomolybdates as Green Catalysts for Aerobic Oxidation

Patel, A.; Pathan, S.

2015, XI, 55 p. 35 illus., 23 illus. in color., Softcover
ISBN: 978-3-319-12987-7